İSTANBUL UNIVERSITY CERRAHPAŞA

ORIGINAL ARTICLE
Electrica 2024; 24(2): 304-317

Intelligent Sliding Mode Control for Quadrotor Trajectory Tracking Under External Disturbances

Nada El Gmili[1], Khadija El Hamidi[2], Mostafa Mjahed[3], Abdeljalil El Kari[4], Hassan Ayad[4]

[1]Laboratory of Materials, Energy, and Control System, Hassan II University, Casablanca, Morocco
[2]Laboratory of Innovation in Management and Engineering for Business (LIMIE), Higher Institute of Engineering and Business (ISGA), Marrakesh, Morocco
[3]Department of Mathematics and Systems, Royal School of Aeronautics, Marrakesh, Morocco
[4]Laboratory of Electrical Systems, Energy Efficiency, and Telecommunications, Cadi-Ayyad University, Marrakesh, Morocco

Cite this article as: N. El Gmili, K. El Hamidi, M. Mjahed, A. El Kari and H. Ayad, "Intelligent sliding mode control for quadrotor trajectory tracking under external disturbances," *Electrica*, 24(2), 304-317, 2024.

ABSTRACT

This paper proposes particle swarm optimization (PSO) and cuckoo search (CS) approaches based on the sliding mode controller (SMC) structure for the unmanned quadrotor's flights. The control law is derived from the Lyapunov theory to guarantee the closed-loop stability. Despite unknown disturbance bounds, the simulation experiments on the nonlinear quadrotor's model prove that these intelligent controllers are very effective for position control, attitude stabilization, automatic take-off and landing, and trajectory tracking missions. Conducted comparisons to the intelligent proportional integral derivative structure through PSO, CS, genetic algorithms, neural networks, fuzzy logic, and some hybrid techniques proposed in previous works of quadrotor control, confirm the superiority of PSO-SMC in terms of robustness and adaptability.

***Index Terms*—**cuckoo search, intelligent control, particle swarm optimization, proportional integral derivative (PID), quadrotor, sliding mode control

Corresponding author:
Nada El Gmili

E-mail:
elgmilinada@gmail.com

Received: September 8, 2023

Revision Requested: October 16, 2023

Last Revision Received: December 15, 2023

Accepted: December 20, 2023

Publication Date: April 17, 2024

DOI: 10.5152/electrica.2024.23101

I	Inertial fixed frame
B	Body frame
R	Rotation matrix
v	Linear velocity
m	Total mass of the quadrotor
F_f	Total thrust
F_k	Force generated by rotor k
F_t	Drag force along x, y and z axes
K_{ftx}, K_{fty} K_{ftz}	Translational drag coefficients
Ω	Angular velocity
M_f	Moment caused by thrust and drag forces following the three rotations
M_a	Moment resulting from aerodynamic friction
K_{fax}, K_{fay} K_{faz}	Coefficients of aerodynamic friction
M_{gh}	Gyroscopic moment of the propellers
J	Inertia of the rotors
U_2, U_3, U_4, U_1	Control inputs
U_x, U_y, U_z	Virtual controls
X	Input vector
u	State vector
s_i(i=1, …, 6)	Sliding surface
e_i	Errors of θ, ψ, x, y, and z
d	Bounded unknown disturbances

$X_i(t)$	Position vector of the particle i in iteration t
$V_i(t)$	Velocity updates vector of the particle i in iteration t
$Pb_i(t)$	Best position of the particle i in iteration t
$Pg\ (t)$	Global best position in iteration t
W	Inertia weight factor
C_1, C_2	Acceleration constants
N	Number of particles in PSO/nests in CS
D	Dimension of search space in PSO/ number of eggs in CS
P_a	Probability of discovered alien eggs
H	Heaviside function
S	Step length
$\alpha > 0$	Step size
Γ	Gamma function
rand	Random variables generated from a uniform distribution in [0, 1]
$Xj(t)$, $Xk(t)$	Two random solutions chosen by random permutation
λ_i^*, k_i^*	Optimal control parameters of sliding mode
ISE	Integral squared error
F	Cost function

I. INTRODUCTION

The evolution of unmanned aerial vehicles (UAVs) requires advanced technologies in order to complete a variety of missions in both civilian and military applications. Although, the use of miniaturized UAVs with vertical take-off and landing (VTOLs) lead to real autonomous navigation capabilities with a reasonable cost and a reduced size. Among the most popular miniaturized VTOL aircrafts, the quadcopter is able to show precise movements, hover at a fixed point, and hover and land vertically in a limited space with a low cost. Thus, this rotary wing vehicle is becoming very attractive and highly required to execute dangerous missions, even in inaccessible environments for humans, for example territorial surveillance, risk assessment of sensitive areas or damage, volcanic study, weather monitoring, area mapping, disaster assessment such as fire detection, research and rescue, infrastructure management (road network, power lines, pipelines, ...), surveillance of sensitive areas such as ports, borders, power plants, railways, and others.

During these missions, robustness of the quadrotor's control algorithm is very important to perfectly achieve precise desired trajectories and stabilized orientations with respect to the physical effects influencing the system dynamics (aerodynamic effects, gravity, gyroscopic effects, friction, and inertia), the intensive coupling (complex nature), and the disturbances effects (wind gusts and other unknown disturbances). To manage this complex and under-actuated system (six degrees of freedom system with only four control inputs), many researchers have designed and implemented linear and nonlinear controllers.

The conventional linear controllers, such as linear quadratic regulator (LQR) and proportional integral derivative (PID) [1, 2], use a linearized model of the nonlinear complex quadrotor model, which can perform the quadrotor's hovering when reduced rotations are required (in the region of the equilibrium point). Due to the simplicity of PIDs' design and tuning, these controllers are considered as the preferred ones in practice [1, 2] and evaluated better than LQR for real-time applications. However, conventional PIDs can lead to poor performance or instability of the quadrotor in situations where nonlinearities and time-varying persist (when performing high aircraft maneuvers). These controllers cannot be robust to face uncertainties or external disturbances as well. Therefore, many researchers have proposed PIDs to perform combinations with other techniques. Advanced algorithms such as soft computing (SC) and swarm intelligence (SI) techniques can ensure good tunings of the PIDs controllers' parameters for each flight mode. These algorithms do not need the linear model of the quadrotor which is considered as a black box, assuming that the inputs and outputs are the only required data at all-time instants. Soft computing controllers as adaptive Neural network (NN) and fuzzy logic (FL) controllers have been applied in [3, 4] to optimize the PID parameters for quadrotor. One of the strongest advantage of NN-based controllers is their learning ability to model nonlinearities and uncertainties independently of the mathematical model. However, such a gains scheduling method of FL-PID controllers has some drawbacks and limitations. The design of FL controllers is based on the perfect choice of the limits, the perfect shaping of the membership functions, and the selection of FL parameters based on the trial and error method, which is not adequate all the time to provide the necessary control actions. These PID-NN controllers have demonstrated good stability and tracking performance even in the presence of disturbances. Adaptive neural network PID-type is proposed for UAVs trajectory tracking in [5]. The nonlinear PID-type is designed in this reference by replacing the integral part of the PID controller of the attitude with a hyperbolic tangent function for the non-modeled dynamics. The problem occurred for stabilizing the positions *x* and *y* that remain oscillating with attitude angles (ϕ, θ, ½). However, the (x, y) plane is under actuated and controllable by the actuated states of the attitude (that are directly controlled). Therefore, this work conclude that parameters computation of roll and pitch controllers constitute the key feature of quadrotor trajectory tracking under external disturbances, demonstrating the superiority of NN PID-type to nonlinear PID-type and other techniques (model-based PID, model-free PID, and nonlinear PID regulator) for obtaining reduced errors.

In the other side, the nonlinear controllers aim to enhance the system's robustness and performance in the presence of uncertainties and disturbances. They are designed to optimize the system's stability and response, particularly in scenarios where traditional linear controllers may be less effective. Among nonlinear controllers, the H∞ controllers use input coupling to avoid the usage of cascade control strategies or augmented state vector through a double integrator [6]. Backstepping controllers are derived based on Lyapunov function, so that the stability of the quadrotor can be guaranteed [7]. In [8], a nonlinear PID-based scheme has been developed inspiring from the SMC for UAVs trajectory tracking problem. The SMC has been also applied by using the hyperbolic tangent function (instead of the sign function) with the same slope as in the proposed nonlinear PID-type structure. Nevertheless, these controllers may fail to guarantee optimal control performance in the presence of unpredictable perturbations from unknown external sources. Thus, auxiliary control effort should be designed to eliminate the effect of the impact of these unpredictable perturbations. In this purpose, nonlinear sliding mode controllers (SMC) are considered powerful and robust to deal with the uncertainties, nonlinearities, and bounded external unknown disturbances effects [9, 10]. This control approach can maintain stability and consistent performance despite modeling imprecisions. Other researchers have combined these controllers to attenuate the effect of unknown external disturbances for quadrotor trajectory tracking problems [11, 12]. For instance, in [12], the proposed hybrid finite-time control (HFTC) method consists of combining finite-time disturbance observer (FDO) with nonsingular terminal sliding mode (NTSM) control to exactly estimate external disturbances, achieving finite-time stability and consequently remarkably superior performance (fast and accurate tracking of the quadrotor). A new approach has been proposed in [11], in accordance with a control law yielded from fractional-order theory, backstepping, and sliding mode methods. In this work, the stability of the system has been ensured in accordance with the Lyapunov stability theory to track different and complex trajectories quickly and accurately, and it has been expressed as the necessity to design an algorithm with more robustness to reduce chattering for actuators and increase stability in practice.

The chattering occurs basically when the control signal changes abruptly and frequently between the two values. Thus, avoiding chattering can be achieved by providing continuous/smooth control signals and retaining the robustness/insensitivity of the control system to bounded model uncertainties and external disturbances. To restrain SMC chattering effects when upper bounds of external disturbances are known, a first solution consists of approximating the discontinuous function by a continuous or a smooth function

(such as sigmoid function) [10]. As a second solution, super twisting SMC technique is employed in order to guarantee the quadrotor stability [13, 14].

To significantly handle the chattering phenomenon in the control signals caused by the discontinuity of the SMC control law and improve at the same time the quadrotor's flight considering unknown dynamics and external disturbances, SMC has been hybridized with controllers based on SC algorithms. In [15], authors proposed Interval Type-2 Adaptive Fuzzy Reaching Sliding Mode System (IT2-AFRSMS), which generates an optimal smooth Adaptive Fuzzy Reaching Sliding Mode Control Law (AFRSMCL) using Interval Type-2-adaptive Fuzzy Systems. Also, NNs are used with adaptive SMC for quadrotor control in [16]. In these works, it has been concluded that it is highly required a good estimation of SMC control law parameters in a reduced computational time, which presents a major problem for nonlinear systems exposed to unknown disturbances effects.

For this objective, it is regarded that SI algorithms can efficiently compute the optimal SMC control law parameters in a reduced computational time as compared to SC algorithms. In [17], a continuous Fast Nonsingular Terminal Sliding Mode Controller based on Linear Extended State Observer (FNTSMC-LESO) is proposed for the quadrotor control under lumped disturbances. Then, the very recent SI algorithm of Fruit Fly Optimization Algorithm has been successfully applied to tune the controllers' parameters for the attitude tracking problem (roll ϕ, pitch θ, and yaw ψ angles' stabilization). Indeed, designing a full control scheme that includes the position control (x, y, and z altitude) is required. The same FNTSMC-LESO controller is proposed, in [18], for a novel cable-driven aerial manipulator applied for aerial tasks. Then, the parameters' tuning of the proposed controller is conducted by an Improved Salp Swarm Igorithm. The simulated cases indicate that the proposed controller achieves a better control effect compared to PID controllers, with lower chattering, higher accuracy, and faster convergence.

The Particle Swarm Optimization (PSO) is considered, as the most successful type of SI, can be proposed in this context thanks to its social behavior patterns that helps to escape from local solutions, ensuring an efficiency computation and a simplicity of implementation [19]. And Cuckoo Search (CS), as a novel SI algorithm, is characterized by the aggressive breeding and egg laying of cuckoo's birds that require few parameters than PSO to converge to good places [20]. Both SI algorithms have been successfully applied for systems' control [21-23] and especially the quadrotor full control [24-26], where it was attested the superiority of PSO to CS algorithm in terms of consumed computational time and performance. The comparisons of results presented in [26] have demonstrated, as well, the competitiveness of PSO to NN for PD/PID controllers optimal tuning.

The main contribution of this work is the development of a full nonlinear control structure for quadrotor allowing to perfectly pursue the desired missions. This approach aims to design robust nonlinear SMC controllers in order to handle the external disturbances' effects without any prior knowledge of their bound. Thus, the quadrotor's control law is derived in the sense of Lyapunov theory to guarantee the closed loop stability. Moreover, PSO and CS algorithms are used to reduce the chattering effects and provide a perfect performance. These SI algorithms can compute intelligently the nonlinear controllers gains in a reduced time as compared to SC algorithms, which makes this approach very suitable for real time applications. To prove the efficiency of the proposed control approach, our work includes as well several simulation experiments conducted on quadrotor including altitude and attitude stabilization, automatic take-off and landing, and trajectory tracking missions. Furthermore, comparisons of intelligent PID based methods to intelligent nonlinear SMC confirm the superiority of the proposed controllers in terms of robustness and adaptability.

The rest of the paper is structured as follows. Section II details the quadrotor dynamic model which is established by using Newton–Euler formalism. Section III proposes the quadrotor full control by using adaptive robust SMC. While section IV presents the intelligent PSO are CS methods and configurations to obtain optimal tuning of SMC parameters. In section V, simulation results are presented, and the last section resumes our conclusions.

II. QUADROTOR DYNAMIC MODELLING

The quadrotor UAV, shown in Fig. 1, has four motors symmetrically disposes in opposed sides of a cross with control electronics in the center. The rotors situated at opposite ends rotate in a synchronized manner, turning in the same direction. In fact, acting cleverly on the rotors' speeds, the aircraft can perform movements of ascent/descent, rolling (by an angle ϕ), pitching (by an angle θ), and yawing (by an angle ψ).

In order to develop the quadrotor dynamical model, a set of reasonable assumptions is considered in this paper:

- Assumption 1: The quadrotor is a rigid body and has a symmetrical structure.
- Assumption 2: Propellers are rigid.
- Assumption 3: Thrust and drag forces proportional to the square of the rotors speed.
- Assumption 4: The quadrotor's center of mass is exactly the body-fixed frame origin.

Let us consider an inertial fixed frame $I=(I_x, I_y, I_z)$ and a body frame $B=(B_x, B_y, B_z)$. The kinematic equations of the translational and

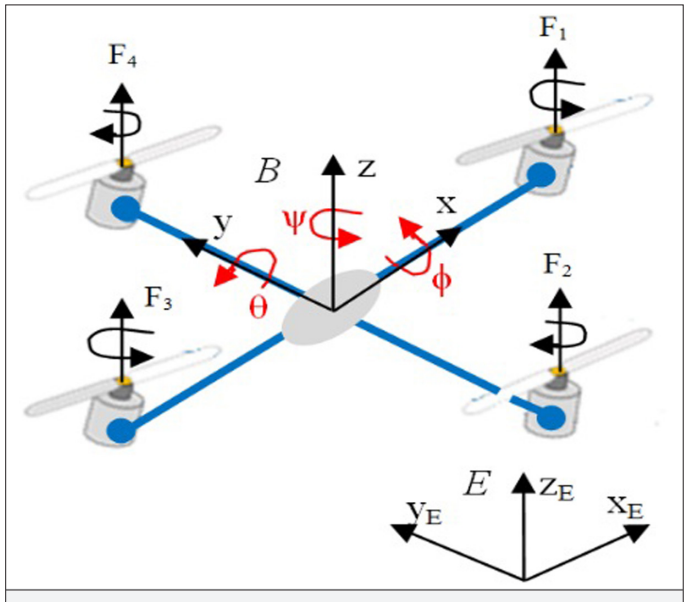

Fig. 1. Quadrotor UAV configuration.

rotational movements are obtained by means of the rotation matrix *R* in (1).

$$R=\begin{pmatrix} c\psi c\theta & s\phi s\theta c\psi - s\psi c\phi & c\phi s\theta c\psi + s\psi c\phi \\ s\psi c\theta & s\phi s\theta s\psi - c\psi c\theta & c\phi s\theta s\psi - s\psi s\phi \\ -s\theta & s\phi c\theta & c\phi c\theta \end{pmatrix} \quad (1)$$

where $c = cos$ and $s = sin$.

The motion equations of quadrotor are derived from Newton–Euler formalism. Therefore, the translational dynamic equations can be expressed as follows.

$$m\dot{v} = R \times F_f + F_t + \begin{pmatrix} 0 & 0 & -mg \end{pmatrix}^T \quad (2)$$

Where *v* is the linear velocity; *m* is the total mass of the quadrotor; F_f is the total thrust force generated by the four rotors with $F_k \approx b\omega_k^2$ is the force generated by the rotor *k*, where ω_k is the rotational speed of rotor *k* and b > 0 is the aerodynamic coefficient of lift.

$$F_f = R \times \begin{pmatrix} 0 & 0 & \sum_{k=1}^{4} F_k \end{pmatrix}^T \quad (3)$$

F_t is the drag force along the axes *x*, *y*, and *z* with K_{ftx}, K_{fty}, and K_{ftz} are the translational drag coefficients.

$$F_t = \begin{pmatrix} -K_{ftx} & 0 & 0 \\ 0 & -K_{fty} & 0 \\ 0 & 0 & -K_{ftz} \end{pmatrix} \times v = \begin{pmatrix} -K_{ftx}\dot{x} \\ -K_{fty}\dot{y} \\ -K_{ftz}\dot{z} \end{pmatrix} \quad (4)$$

The rotational dynamic equations of quadrotor can be obtained according to equation (5).

$$J\dot{\Omega} = M_f - M_{gh} - M_a - \Omega \times J\Omega \quad (5)$$

Where Ω is the angular velocity expressed in the fixed reference.

$$\Omega = \begin{pmatrix} 1 & 0 & -s\theta \\ 0 & c\phi & s\phi \\ 0 & -s\phi & c\phi c\theta \end{pmatrix} \times \begin{pmatrix} \dot{\phi} \\ \dot{\theta} \\ \dot{\psi} \end{pmatrix} \quad (6)$$

$J = \begin{pmatrix} I_x & 0 & 0 \\ 0 & I_y & 0 \\ 0 & 0 & I_z \end{pmatrix}$ is the inertia of the system.

M_f is the moment caused by the thrust and the drag forces following the three rotations, with $D_k \approx d\omega_k^2$ is the drag force generated by the rotor *k*, $d > 0$ is drag coefficient that depends on the geometry of the propeller and the fluid density of the medium (air in this case, and *l* is the length of the arm between the rotor and the quadrotor's center of gravity).

$$M_f = \begin{pmatrix} lb(\omega_4^2 - \omega_2^2) \\ lb(\omega_3^2 - \omega_1^2) \\ d(\omega_1^2 - \omega_2^2 + \omega_3^2 - \omega_4^2) \end{pmatrix} \quad (7)$$

M_a is the moment resulting from aerodynamic friction with K_{fax}, K_{fay}, and K_{faz} are coefficients of aerodynamic friction.

$$M_a = \begin{pmatrix} -K_{fax} & 0 & 0 \\ 0 & -K_{fay} & 0 \\ 0 & 0 & -K_{faz} \end{pmatrix} \times \Omega^2 \quad (8)$$

M_{gh} is the gyroscopic moment of the propellers with J_r is the inertia of the rotors, ω_i is the rotational speed of the rotor *i*, and $\Omega_r = \omega_1 - \omega_2 + \omega_3 - \omega_4$;

$$M_{gh} = \sum_{i=1}^{4} \Omega \wedge J_r \times \begin{pmatrix} 0 & 0 & (1)^{i+1}\omega_i \end{pmatrix}^T \quad (9)$$

Thus, the dynamic model of the quadrotor in terms of rotation (ϕ, θ, ½) and position (*x*, *y*, *z*) is expressed as follows [27]:

$$I_x\ddot{\phi} = \left(-\dot{\theta}s\phi + \dot{\psi}c\phi c\theta\right)\left(\dot{\theta}c\varphi + \dot{\psi}c\theta c\phi\right)\left(I_y - I_z\right) - \left(\dot{\theta}c\phi + \dot{\psi}c\theta s\phi\right)J_r\Omega_r - \left(\dot{\phi}^2 - 2\dot{\phi}\dot{\psi}s\theta\dagger\right)k_{fax} + l\,U_2 \quad (10)$$

$$I_y\ddot{\theta} = \left(\dot{\psi}c\phi c\theta - \dot{\theta}s\phi\right)\left(\dot{\phi} - \dot{\psi}s\theta\right)\left(I_z - I_x\right) - \left(\dot{\psi}s\theta - \dot{\phi}\right)J_r\Omega_r - \left(\dot{\theta}^2c\phi^2 + 2\dot{\theta}\dot{\psi}c\theta s\phi\, c\varphi + \dot{\psi}^2c\theta^2\, s\phi^2\right)k_{fay} + l\,U_3 \quad (11)$$

$$I_z\ddot{\psi} = \left(\dot{\psi}\, s\phi c\theta + \dot{\theta}c\phi\right)\left(\dot{\phi} - \dot{\psi}s\theta\right)\left(I_x - I_y\right) - \left(\dot{\theta}^2\, s\phi^2 - 2\,\dot{\theta}\dot{\psi}c\theta s\phi c\phi + \dot{\psi}^2c\theta^2c\phi^2\right)k_{faz} + U_4 \quad (12)$$

$$m\ddot{x} = \left(c\psi s\theta c\phi + s\psi s\phi\right)U_1 - k_{ftx}\dot{x} \quad (13)$$

$$m\ddot{y} = \left(s\psi s\theta c\phi - c\psi s\phi\right)U_1 - k_{fty}\dot{y} \quad (14)$$

$$m\ddot{z} = -mg + \left(c\theta c\phi\right)U_1 - k_{ftz}\dot{z} \quad (15)$$

where the control inputs are given by equation (16).

$$\begin{cases} U_1 = b\,(\omega_1^2 + \omega_2^2 + \omega_3^2 + \omega_4^2) \\ U_2 = b\,(\omega_4^2 - \omega_2^2) \\ U_3 = b\,(\omega_3^2 - \omega_1^2) \\ U_4 = d\,(\omega_1^2 - \omega_2^2 + \omega_3^2 - \omega_4^2) \end{cases} \quad (16)$$

III. ADAPTIVE ROBUST SLIDING MODE CONTROL SYSTEM

To manage the quadrotor dynamics, it is considered in small rotations ($cos\ x = 1$, $sin\ x = 0$). Then, the equations (10–15) become as defined in [, 27]:

$$\ddot{\phi} = \frac{l}{I_x}U_2 + \dot{\psi}\dot{\theta}\frac{I_y - I_z}{I_x} + d_1 \quad (17)$$

$$\ddot{\theta} = \frac{l}{I_y}U_3 + \dot{\phi}\dot{\psi}\frac{I_z - I_x}{I_y} + d_2 \quad (18)$$

$$\ddot{\psi} = \frac{1}{I_z}U_4 + \dot{\phi}\dot{\theta}\frac{I_x - I_y}{I_z} + d_3 \quad (19)$$

$$\ddot{x} = \frac{c\psi s\theta c\phi + s\psi s\phi}{m} U_1 - \frac{k_{ftx}}{m}\dot{x} + d_4 \tag{20}$$

$$\ddot{y} = \frac{s\psi s\theta c\phi - c\psi s\phi}{m} U_1 - \frac{k_{fty}}{m}\dot{y} + d_5 \tag{21}$$

$$\ddot{z} = -g + \frac{c\theta c\phi}{m} U_1 - \frac{k_{ftz}}{m}\dot{z} + d_6 \tag{22}$$

where d_i *(i=1, …, 6)* represent non-modeled or neglected dynamics of system (10–15) and unknown external disturbances.

Consequently, it can be clearly observed from these equations (17–22) that the quadrotor is an under-actuated system with six outputs (ϕ, θ, ψ, *x*, *y*, *z*) and only four control inputs (U_2, U_3, U_4, U_1). Thus, the controls U_2, U_3, and U_4 can be designed as control inputs for roll (ϕ), pitch (θ), and yaw (ψ) angles, respectively. However, it can be noticed that ϕ, θ, and U_1 affect the positions *x*, *y*, and *z*. To control each of these outputs separately, the three virtual control inputs U_x, U_y, U_z can be used to compute the desired angles of roll (ϕ_d) and pitch (θ_d), which can achieve indirectly the positions' trajectories. The virtual controls are given by equation (23), and the desired roll and pitch angles' trajectories are represented by equation (24).

$$\begin{cases} U_x = \left(c\psi\, s\theta\, c\phi + s\psi\, s\phi\right) U_1 \\ U_y = \left(s\psi\, s\theta\, c\phi - c\psi\, s\phi\right) U_1 \\ U_z = c\theta\, c\phi U_1 \end{cases} \tag{23}$$

$$\begin{cases} \phi_d = arc\sin\left(\dfrac{U_x s\psi_d - U_y c\psi_d}{\sqrt{U_x^2 + U_y^2 + U_z^2}}\right) \\ \theta_d = \arctan\left(\dfrac{U_x c\psi_d + U_y s\psi_d}{U_z}\right) \end{cases} \tag{24}$$

The state vector is defined to be $\underline{X} = [X^T \dot{X}^T]^T$. Then, the dynamic model (17–22) with consideration of unknown and unpredictable disturbances can be simplified as follows:

$$\ddot{X} = f(X) + g(X)u + d \tag{25}$$

where *X*, *u*, and *d* are, respectively, the input, the state, and the bounded unknown disturbances.

$$X = \left[X_1 X_2 X_3 X_4 X_5 X_6\right]^T = \left[\phi\, \theta\, \psi\, x\, y\, z\right]^T \tag{26}$$

$$u = \left[u_1 u_2 u_3 u_4 u_5 u_6\right]^T = \left[U_2 U_3 U_4 U_x U_y U_z\right]^T \tag{27}$$

$$d = \left[d_1 d_2 d_3 d_4 d_5 d_6\right]^T \tag{28}$$

The nonlinear dynamic function *f(X)* and nonlinear control function *g(X)* matrices are represented by the following equations:

$$f(X) = \left(f_1 f_2 f_3 f_4 f_5 f_6\right)^T = \left(\dot{\psi}\dot{\theta}a_1 \quad \dot{\phi}\dot{\psi}a_2 \quad \dot{\theta}\dot{\phi}a_3 \quad 0 \quad 0 \quad -g\right)^T \tag{29}$$

$$g(X) = \begin{pmatrix} b_1 & 0 & 0 & 0 & 0 & 0 \\ 0 & b_2 & 0 & 0 & 0 & 0 \\ 0 & 0 & b_3 & 0 & 0 & 0 \\ 0 & 0 & 0 & b_4 & 0 & 0 \\ 0 & 0 & 0 & 0 & b_5 & 0 \\ 0 & 0 & 0 & 0 & 0 & b_6 \end{pmatrix} \tag{30}$$

$$a_1 = \frac{J_y - J_z}{J_x}, a_2 = \frac{J_z - J_x}{J_y}, a_3 = \frac{J_x - J_y}{J_z},$$

with the abbreviations $b_1 = \frac{l}{J_x}, b_2 = \frac{l}{J_y}, b_3 = \frac{1}{J_z}, b_4 = b_5 = b_6 = \frac{1}{m}$.

The control objective is to direct a state trajectory *X* towards a desired reference trajectory $X_d = [X_{1d}\, X_{2d}\, X_{3d}\, X_{4d}\, X_{5d}\, X_{6d}]^T$ despite the presence of unknown disturbances. Fig. 2. Illustrates the developed diagram for the entire quadrotor's control by using SMC. The bloc "Position controllers" consists of three controllers for position (*x, y, z*) and the bloc "Angles controllers" consists of controllers for angles (ϕ, θ, ψ).

For improving the autonomous flight capability, the desired signals for position and yaw angle (x_d, y_d, z_d, ψ_d) are fixed by user. Then, sensor signals (desired roll ϕ_d and desired pitch θ_d) are automatically processed by program with the aim of ensuring the quadrotor's stability.

A. Robust Sliding Mode Control System

The SMC is a robust control method capable to ensure position *x(t), y(t), z(t),* and orientation $\phi(t)$, $\theta(t)$, $\psi(t)$ steer the desired trajectory $x_d(t)$, $y_d(t)$, $z_d(t)$, $\phi_d(t)$, $\theta_d(t)$, $\psi_d(t)$ asymptotically for the quadrotor. To demonstrate the stability of the proposed controllers, the stability of the closed loop will be analyzed in three steps.

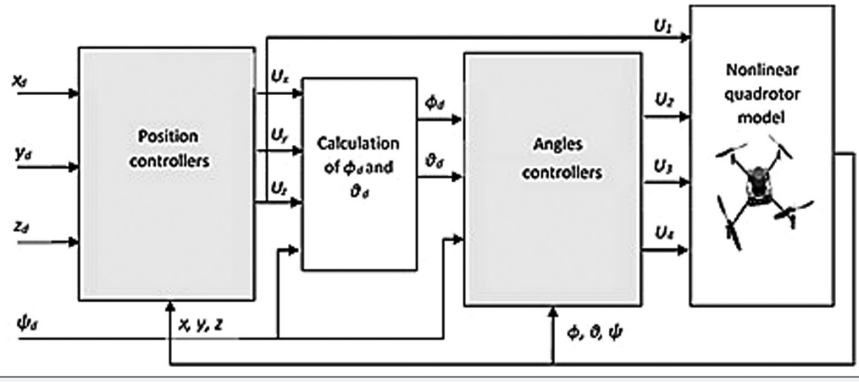

Fig. 2. Complete control scheme for quadrotor.

The first step in designing the SMC is to consider the tracking error and its derivative first.

$$e = \left[e_1 e_2 e_3 e_4 e_5 e_6\right]^T = X - X_d, \dot{e} = \dot{X} - \dot{X}_d \tag{31}$$

Then, the sliding surface can be defined as [14].

$$s\left(\underline{X}, t\right) = \left[s_1 s_2 s_3 s_4 s_5 s_6\right]^T \tag{32}$$

$$s_i = \dot{e}_i + \lambda_i e_i, i = 1, ..., 6 \tag{33}$$

Considering equation (25), the time derivative of the sliding surface can be obtained as follows:

$$\dot{s}_i = \ddot{e}_i + \lambda_i \dot{e}_i = \left(f_i + b_i u_i + d_i\right) - \ddot{x}_{di} + \lambda_i \dot{e}_i \tag{34}$$

For the second step, the following Lyapunov function is considered

$$V_i\left(s_i\right) = \frac{1}{2} s_i^2 \tag{35}$$

According to the exponential reaching law, the time derivative of the sliding surface satisfying ($ss < 0$) is written as the following:

$$\dot{s}_i = \lambda_i \dot{e}_i + \ddot{x}_i - \ddot{x}_{di} = \lambda_i \dot{e}_i + f_i + b_i u_i + d_i = u_{sli} = -k_i sign\left(s_i\right) - \lambda_i s_i \tag{36}$$

Clearly, by adding the potential rate terms $-\lambda_i s_i$ (with $\lambda i > 0, \forall I \in [,6]$), the state is forced to approach the switching manifolds faster when s_i is large.

The time derivative of equation (35) yields:

$$\dot{V}_i\left(s_i\right) = s_i \dot{s}_i = s_i\left(\lambda_i \dot{e}_i - \ddot{x}_{di} + f_i + b_i u_i + d_i\right) \tag{37}$$

Concerning the third step, a SMC can be obtained as follows.

$$u_i = \frac{1}{b_i}\left(-f + \ddot{x}_{di} - k_i sign\left(s_i\right) - 2\lambda_i \dot{e}_i - \lambda_i^2 e_i\right) \tag{38}$$

Substituting equation (37) into equation (38) gives:

$$\dot{V}_i\left(s_i\right) = s_i u_{sli} + d_i s_i = -\lambda_i s_i^2 - k_i s_i sign\left(s_i\right) + d_i s_i = -\lambda_i s_i^2 - k_i \left|s_i\right| + d_i s_i \tag{39}$$

To guarantee to closed loop stability using this Lyapunov based method, $\dot{V}_i$ must be negative definite. Thus, the system's trajectory can be driven towards the sliding surface and can be stayed on it ntil the origin is reached asymptotically. Hence, the controllers' parameters should be chosen such that $\dot{V}_i \le 0$ is always satisfied. Let us assume that d_i is bounded with δ_i. In order to ensure $\left(\dot{V}_i \le 0\right)$, the optimal parameters (k_i^* and λ_i^*) should be well chosen. Consequently λ_i^* must be positive semi-definite and $\left(-k_i^* \left|s_i\right| + \delta_i s_i\right)$ must negative semi-definite, which can be guaranteed by choosing $\left(k_i^* \ge \delta_i\right)$ and $\left(\lambda_i^* \ge 0\right)$.

B. Adaptive Robust Sliding Mode Control System

Despite imprecise knowledge of external disturbances bounds and all physical parameters that affect quadrotor dynamics, the adjustments of SMC parameters can guarantee the system stability. The adaptation law is derived using the following augmented Lyapunov function:

$$V_i'\left(s_i, \lambda_i, k_i\right) = V_i\left(s_i\right) + \frac{1}{2\gamma\lambda_i}\tilde{\lambda}_i^2 + \frac{1}{2\gamma\lambda_i}\tilde{k}_i^2 \tag{40}$$

The online optimal estimations of λ_i and k_i that ensure the best tracking control performance of the quadrotor (8) by providing optimal parameters λ_i^* and k_i^* allow the perturbations d_i to be efficaciously rejected while simultaneously avoiding the undesired chattering, with $\tilde{\lambda}_i = \lambda_i - \lambda_i^*$, $\tilde{k}_i = k_i - k_i^*$, $\gamma_{\lambda i}$, and γ_{ki} are gains adaptation.

The time derivative of the above equation is:

$$\dot{V}_i'\left(s_i, \lambda_i, k_i\right) = \dot{V}_i\left(s_i\right) + \frac{1}{\gamma\lambda_i}\tilde{\lambda}_i\left(\dot{\lambda}_i\right) + \frac{1}{\gamma k_i}\tilde{k}_i\left(\dot{k}_i\right) \tag{41}$$

Substituting equation (39) into equation (41) gives:

$$\dot{V}_i'\left(s_i, \lambda_i, k_i\right) = \left(s_i u_{sli} + d_i s_i\right) + \frac{1}{\gamma\lambda_i}\tilde{\lambda}_i\left(\dot{\lambda}_i\right) + \frac{1}{\gamma k_i}\tilde{k}_i\left(\dot{k}_i\right) \tag{42}$$

Then, by replacing u_{sli} according to the expression of the estimated $\breve{u}_{sli} = u_{sli} - u_{sli}^*$, with the optimal $u_{sli}^* = -\lambda_i^* s_i - k_i^* sign\left(s_i\right)$.

$$\begin{aligned}
\dot{V}_i'\left(s_i, \lambda_i, k_i\right) &= s_i\left(\hat{u}_{sli} + u_{sli}^* + \delta_i\right) + \frac{1}{\gamma\lambda_i}\tilde{\lambda}_i\dot{\lambda}_i + \frac{1}{\gamma k_i}\tilde{k}_i\dot{k}_i \\
&= s_i\hat{u}_{sli} + s_i\left(u_{sli}^* + \delta_i\right) + \frac{1}{\gamma\lambda_i}\tilde{\lambda}_i\dot{\lambda}_i + \frac{1}{\gamma k_i}\tilde{k}_i\dot{k}_i \\
&= s_i\left(-\hat{\lambda}_i s_i - \hat{k}_i sign\left(s_i\right)\right) + s_i\left(u_{sli}^* + \delta_i\right) + \frac{1}{\gamma\lambda_i}\tilde{\lambda}_i\dot{\lambda}_i + \frac{1}{\gamma k_i}\tilde{k}_i\dot{k}_i \\
&= s_i\left(u_{sli}^* + \delta_i\right) + \tilde{\lambda}_i\left(\frac{\dot{\lambda}_i}{\gamma\lambda_i} - s_i^2\right) + \tilde{k}_i\left(\frac{\dot{k}_i}{\gamma k_i} - \left|s_i\right|\right)
\end{aligned} \tag{43}$$

The value of $\dot{V}_i'$ can remain negative if $\left(\frac{1}{\gamma_{ki}}\dot{k}_i - \left|s_i\right| = 0\right)$ and $\left(\frac{\dot{\lambda}_i}{\gamma_{\lambda i}} - s_i^2 = 0\right)$. Thus, to ensure the adaptation law $\dot{k}_i = \gamma_{ki}\left|s_i\right|$ and $\dot{\lambda}_i = s_i^2\gamma_{\lambda i}$, the optimal parameters k_i^* and λ_i^* should be well chosen to guarantee the stability of the system (10–15) even the presence of unknown disturbances and some non modeled dynamics. Therefore, equation (43) becomes as follows.

$$\dot{V}_i'\left(s_i, \lambda_i, k_i\right) = -\lambda_i^* s_i^2 - k_i^*\left|s_i\right| + \delta_i s_i \tag{44}$$

Therefore, the value of $\left(\delta_i - k_i^*\right)$ can remain negative if the condition $\left(\delta_i - k_i^* = -\varepsilon\right)$, is satisfied where ($\mathcal{E} > 0$). For this purpose, two SI algorithms will be configured in the next section in order to automatically compute (online) the optimal parameters $\left(k_i^* \text{ and } \lambda_i^*\right)$ for an autonomous flight stabilization of the nonlinear quadrotor's model (10–15). To establish the convergence of the tracking errors, as well as the stability of the closed loop, both algorithms consider the fitness function that must ensure no oscillations (overshoot around 0%) and achieve the system stabilization in a reasonable settling time for the six outputs taking into consideration these conditions $\left(k_i^* \ge \delta_i\right)$ and $\left(\lambda_i^* \ge 0\right)$. Consequently, if this function is chosen as the quadratic error between the desired and actual outputs, the proposed SI algorithms will seek over iterations to reduce the static or the dynamic errors that convergence to zero when t → ∞, ensuring the convergence of the control law u_{sli} to u_{sli}^*.

IV. OPTIMAL SLIDING MODE CONTROL SYSTEM

In order to achieve enhanced control performance for the nonlinear and fully coupled quadcopter model described by equations (10–15), a rigorous optimization process becomes imperative. Considering an amount of initial solutions, computer capacity can perform lot iterations and use the information gained to optimize variations and reach global optimum for an optimal control. Given a set of initial solutions, the computational capacity of computers allows for numerous iterations to optimize adjustments of potential solutions (controllers' parameters), ultimately reaching the global optimum for an optimal quadrotor's full flight. The optimization methods of PSO and CS are applied for this purpose in order to seek online the best SMC parameters for the quadcopter's outputs (roll ϕ, pitch θ, yaw ψ, position x, position y, altitude z).

A. Overview of Particle Swarm Optimization

Particle Swarm Optimization is a class of stochastic algorithms developed for solving hard optimization problems. It is inspired by the collective intelligence through social interactions of animals moving in swarm like bird flocking [19].

The particles in PSO refer to points in the search space that changes their positions X_i (t) in iterations (t) based on velocities updates V_i (t). Initially, the initial swarm positions and velocities are randomly dispersed. Then, each particle "i" in PSO tries to improve its quality (fitness) following three rules. First, it tends to follow the direction of its current velocity. Second, it tends to move toward the memorized personal best experience it has ever visited $Pb_i(t+1)$, calculated according to (44). Finally, it tends to move towards the successful neighbor's position $Pg\ (t+1)$, which is the position of the particle that has the smallest fitness value in the swarm as given by (45). In fact, the three rules that affect the new search direction are incorporated in the velocities update formula as shown in (46) with three weighting factors w, C_1, and C_2. The velocity formula includes also the uniformly distributed random variable *rand* that takes values in [0, 1]. The position of each particle in the swarm is updated according to (47) for the next generation ($t+1$).

$$Pb_i\ (t+1)=\begin{cases} X_i\ (t+1) & \text{if } f\ (X_i\ (t+1)) < f\ (Pb_i\ (t)) \\ Pb_i\ (t) & \text{else} \end{cases} \tag{44}$$

$$Pg = min_{i=1,2....N}{}^{f\ (Pb_i\ (t+1))} \tag{45}$$

$$V_i\ (t+1) = w.V_i\ (t) + C_1 rand.(Pb_i\ (t) - X_i\ (t)) + C_2.rand.(Pg_i\ (t) - X_i\ (t)) \tag{46}$$

$$X_i\ (t+1) = X_i\ (t) + V_i\ (t+1) \tag{47}$$

B. Overview of Cuckoo Search

Cuckoo Search Optimization algorithm draws inspiration from the life of cuckoo birds, as introduced by Yang and Deb in 2009. It mimics the distinctive breeding and reproductive behavior of these birds, which forms the basic characteristics of CS. In this process, adult cuckoos lay eggs in the habitat of other host birds and the eggs that remains undiscovered by host birds grow and develop to mature cuckoos. Consequently, groups of cuckoos gradually migrate to better locations, converging during their journey [20].

Cuckoo Search algorithm involves N nests (habitats), each containing D eggs. The performance of these nests is evaluated using a cost function F, which is applied to the habitat as an array of size $1 \times D$. Some of these alien eggs are discovered with probability P_a from [0, 1], are replaced by new random solutions [20]. This fraction of new solutions is calculated based on equation (48).

$$X_i(t+1) = X_i(t) + H(P_a - r)\left(X_j(t) - X_k(t)\right) \tag{48}$$

Rather than employing a straightforward random walk, the CS algorithm adopts Lévy flights mechanism when cuckoos move to find the best environment. This mechanism determines the step length, denoted S, as outlined in equation (49). S is derived using Mantegna algorithm, which relies on a Gaussian normal distribution, where σu^2 represents the variance of this distribution, as specified in equation (50). The update of the new solution $X_i\ (t+1)$ for cuckoo i is computed according to equation (51).

$$Lévy(\lambda) \approx S = Norm\left(0, \sigma_u^2\right) * \left|Norm(0,1)\right|^{-1/\lambda} \qquad (1 < \lambda \le 3) \tag{49}$$

$$\sigma_u^2 = \left\{ \frac{\Gamma(1+\lambda)\sin(\pi\lambda/2)}{\Gamma\left[(1+\lambda)/2\right]\lambda 2^{(\lambda-1)/2}} \right\}^{1/\lambda} \tag{50}$$

$$X_i(t+1) = X_i(t) + \alpha.\text{Lévy}(\lambda) \tag{51}$$

where Γ is the gamma function; $\alpha > 0$ is the step size; R and r are random variable generated from a uniform distribution in the interval [0, 1]; $Xj\ (t)$ and $Xk(t)$ are two random solutions chosen by random permutation; and H is a Heaviside function.

C. Optimal Sliding Mode Control System

In the preceding section, controllers are developed according to equation (38) with the objective of stabilizing the overall system. As mentioned earlier, a total of 12 control parameters must be chosen simultaneously for the six controllers. To achieve this, PSO and CS are used online to determine the optimal values for these controllers' parameters ($\lambda_1^*, \lambda_2^*, \lambda_3^*, \lambda_4^*, \lambda_5^*, \lambda_6^*, k_1^*, k_2^*, k_3^*, k_4^*, k_5^*, k_6^*$).

The initial matrices are generated within a search space ranging from 0 to 50, with a dimension of $D = 12$ (representing 12 parameters). A number of particles (for PSO) or nests (for CS) equal to 200 is used for this purpose. To assess the effectiveness of the quadrotor's responses obtained using intelligent sliding mode controllers, the fitness needs to ensure that the responses are fast, precise, and robust. To minimize the disparities between the desired and the controlled responses, the optimization performance metric used to evaluate the fitness function is the Integral Square Error (ISE), as defined in equation (52). Prior researches [22, 25-26] has demonstrated that the ISE index offers superior performance when evaluating the control system compared to other performance indices based on integrating a positive term associated with the error: The Integral Absolute Error, the Integral Time Absolute Error, and the Integral Time Square Error.

$$\text{ISE} = \int_0^\infty e^2(t)dt \tag{52}$$

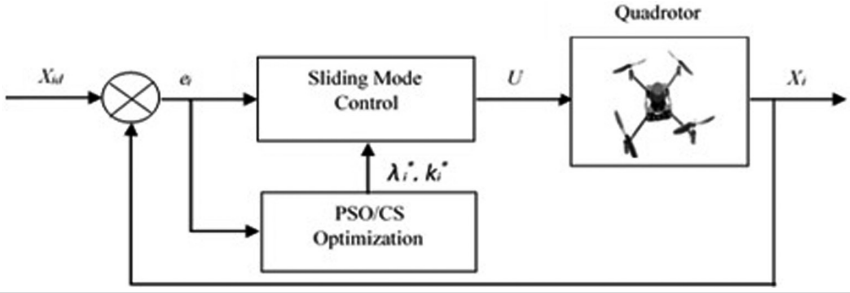

Fig. 3. Block diagram of the robust optimal SMC system using PSO or CS.

Given that the system involves six controllers, a vector of ISEs can be represented as $ISE_s=[ISE_1, ISE_2, ISE_3, ISE_4, ISE_5, ISE_6]$ corresponding to roll, pitch, yaw, longitude, latitude, and altitude, respectively. For all six controllers, both CS and PSO algorithms aim to minimize the fitness function described in equation (53).

$$F = \sum_{s=1}^{6} ISE_s \tag{53}$$

The fitness function is computed by simulating the quadrotor's dynamic model over a time span of $t = 20$ seconds. Fig. 3 represents the block diagram used to determine the optimal set of the controllers' parameters (λ_i^*, k_i^*, with $i=\{1,2,3,4,5,6\}$).

Within the PSO algorithm, the parameters that govern the exploration capacity of each particle are the inertia weight "*w*" and the confidence coefficients C_1 and C_2. A balance between local and global exploration is achieved when setting $w = 0.8$. Values of $C_1 = 0.8$ and $C_2 = 1.2$ are selected to prevent rapid convergence while placing more trust in the global best position Pg. In contrast, in the CS algorithm, the parameter λ remains constant at 1.5, as indicated in previous studies [22, 25, 26]. Last, the stopping criterion is determined by setting the maximum number of iterations, denoted as *G*, to *20*. This choice is made to retain the particle (or nest) with the best fitness value.

V. SIMULATION RESULTS

The experiment simulations involving the quadcopter aim to showcase the efficacy of both PSO and CS algorithms in stabilizing the quadrotor. These tests are conducted under two scenarios: one involves the quadrotor hovering at a fixed point, and the other simulates hovering and landing during tracking missions. To achieve this, both algorithms are implemented online within the MATLAB/SIMULINK environment to seek optimal parameters for SMC structure relied to the quadrotor model. This enables a real-time search for the optimal parameters, which are subsequently evaluated. Table I provides the model parameters' values of the quadrotor system.

A. Hovering with Attitude Stabilization

This simulation tests a hovering scenario for the quadrotor, where the initial system conditions and desired states are set as follow: $X_0=[\phi_0\ \theta_0\ \psi_0\ x_0\ y_0\ z_0]=[0^\circ\ 0^\circ\ 0^\circ\ 0m\ 0m\ 0m]$ and $X_d=[\phi_d\ \theta_d\ \psi_d\ x_d\ y_d\ z_d]=[\phi_d\ \theta_d\ 5^\circ\ 1m\ 2m\ 2m]$.

Essentially, the objective is for the controllers to maintain the quadrotor at a specific position $(x_d\ y_d\ z_d)=(1m\ 2m\ 2m)$ while yawing at an orientation angle ranging from 0° to 5°. The computation of the desired roll angle (ϕ_d) and pitch angle (θ_d) is linked to the outputs of *x* and *y* controllers (U_x and U_y). Consequently, their desired values are influenced by these controllers' outputs. In this simulation, the best values for the twelve controllers' parameters ($\lambda_1^*, \lambda_2^*, \lambda_3^*, \lambda_4^*, \lambda_5^*, \lambda_6^*, k_1^*, k_2^*, k_3^*, k_4^*, k_5^*, k_6^*$) are determined according to Table II. The resulting control signals $u_1, ..., u_4$ are depicted in Fig. 4, and the obtained results are visualized at Fig. 5.

Table III provides an overview of the intelligent SMC performance obtained using PSO and CS, including metrics such settling time (T_s), maximum overshoot (M_p), Root Mean Squared (RMS) Error, and ISE. Additionally, the table offers a comprehensive analysis by comparing the performance of PID controllers achieved by PID controllers based neural network (GS-NNPID) [4], PSO (PSO-PID) [26], cooperative PSO-CS (PSO-CS-PID) [26], and genetic algorithms (GAHC-PID) [28].

As depicted in Fig.4, the rotors require a significant amount of energy to counteract gravitational effects. The figure indicates that during the startup phase, the control laws of PSO-SMC (representing the

TABLE I. THE PARAMETERS OF THE QUADCOPTER MODEL [27]

Parameter	Value
I_x	7.5 10^{-3} kg.m^2
I_y	7.5 10^{-3} kg.m^2
I_z	1.3 10^{-3} kg.m^2
K_{fax}	5.567 10^{-4} N/rad/s
K_{fay}	5.567 10^{-4} N/rad/s
K_{faz}	6.354 10^{-4} N/rad/s
K_{ftx}	5.567 10^{-4} N/rad/s
K_{fty}	5.567 10^{-4} N/rad/s
K_{ftz}	6.354 10^{-4} N/rad/s
g	9.806 m/s
J_r	2.8385 10^{-5} kg.m^2
b	2.9842 10^{-5} kg.m.rad^{-2}
d	3.232 10^{-6} kg.m.rad^{-2}
m	0.65 kg
l	0.23 m

TABLE II. OPTIMAL SMC PARAMETERS OBTAINED WITH PSO AND CS FOR THE QUADROTOR

Quadrotor's Output	Optimal Parameter	Optimization Method	
		PSO	*CS*
ϕ	k_1^*	0.54350	5.476
	λ_1^*	67.50988	218.712
θ	k_2^*	0.00001	13.679
	λ_2^*	42.66285	108.118
ψ	k_3^*	5.33146	2.708
	λ_3^*	42.07678	30.254
x	k_4^*	0.00001	0.294
	λ_4^*	2.85765	13.932
y	k_5^*	0.00001	0.541
	λ_5^*	2.43910	3.378
z	k_6^*	0.33234	0.078
	λ_6^*	3.09832	2.867

CS, cuckoo search; PSO, particle swarm optimization.

speeds of the four rotors) move up, followed by smoother variations as the quadrotor stabilizes. These results confirm the capacity of PSO to reduce significantly the chattering phenomenon.

Analyzing Fig. 5 and Table III, it becomes evident that the nonlinear SMC controllers tuned using PSO exhibit superior performance compared to those tuned with CS. Particle swarm optimization demonstrates fast responses (reduced settling times) with no overshoot observed for position (*x, y, z*) and yaw attitude (ψ). In [8], the adopted gain selection criterion take into consideration the energy consumption so that the RMS value of each signal $u_{i=}(i=1, \ldots, 4)$ fell within a range of variation of ± 5% of the corresponding RMS values produced by the PID-based and the SMC controllers. The provided RMS values by using the proposed nonlinear PID-based (NL PID in Table III) controller are attested reduced to both SMC and PID-based when the system is undisturbed. As compared to our results, the nonlinear PID-based have performed reduced RMS values except for the tracking error for roll and pitch angles that are found equal to 0.8205 and 1.0532 [8], respectively. Therefore, PSO results here better system dynamics for roll and pitch angles. In contrast, when considering the results obtained with CS, a slight overshoot of 2% is noticeable in the longitude *x,* and notable variations (oscillations) are observed in the roll and pitch angles. The observed oscillations can be attributed to the control law variations associated with CS-SMC, as depicted in Fig. 4. These findings confirm that parameters computation of roll and pitch controllers is the key feature of quadrotor trajectory tracking as concluded in [5].

As illustrated in Table III, the PSO-SMC results performances near to those of PSO-CS-PID and PSO-PID [26], in terms of optimal quadrotor control, characterized by fast settling times, absence of overshoot, and minimized ISE values. A comparison between PSO-SMC and the hierarchical GAHC-PID structure developed in [28], for a hovering quadrotor to position coordinates (10*m*, 10*m*, 10*m*), reveals significant reductions in settling times from 2.2*s*, 2.5*s*, and 2.5*s* to 1.29*s*, 1.28*s*, and 1.07*s* for position *x, y,* and *z*, respectively. These findings underscore the superior exploration of optimal responses achieved by PSO-SMC.

The proposed GS-NNPID in [4] has exhibited remarkable performance compared to the proposed fuzzy PID controllers (FPID) and Fuzzy particle swarm optimization (FPID-PSO) as presented in [3]. Thus, the comparison of PSO-SMC to GS-NNPID shows in the same table a noteworthy reduction in settling time for *x*, *y*, and *z*, where they decrease to 1.29 s, 1.28 s, and 1.07 s, from 1.36 s, 1.5 s, and 4.7 s. Consequently, the PSO-SMC demonstrates a higher level of precision and follow perfectly sensor signals for desired roll and pitch angles (ϕ_d and θ_d), coupled with minimized ISE values.

B. Trajectory Tracking with/without Disturbances Injection

This simulation assesses the quadrotor's ability to track a desired circular trajectory, while it hovers, maintain a stable attitude, and performs a landing maneuver with a 5° yaw movement. Additionally, external disturbances effects are introduced in the six

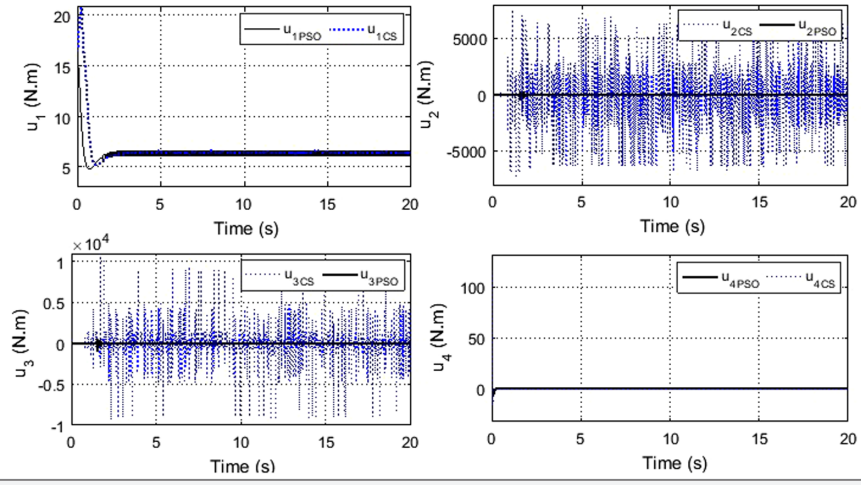

Fig. 4. PSO-SMC controls (u_{1PSO}, u_{2PSO}, u_{3PSO}, u_{4PSO}) and CS-SMC controls (u_{1CS}, u_{2CS}, u_{3CS}, u_{4CS}) for hovering quadrotor.

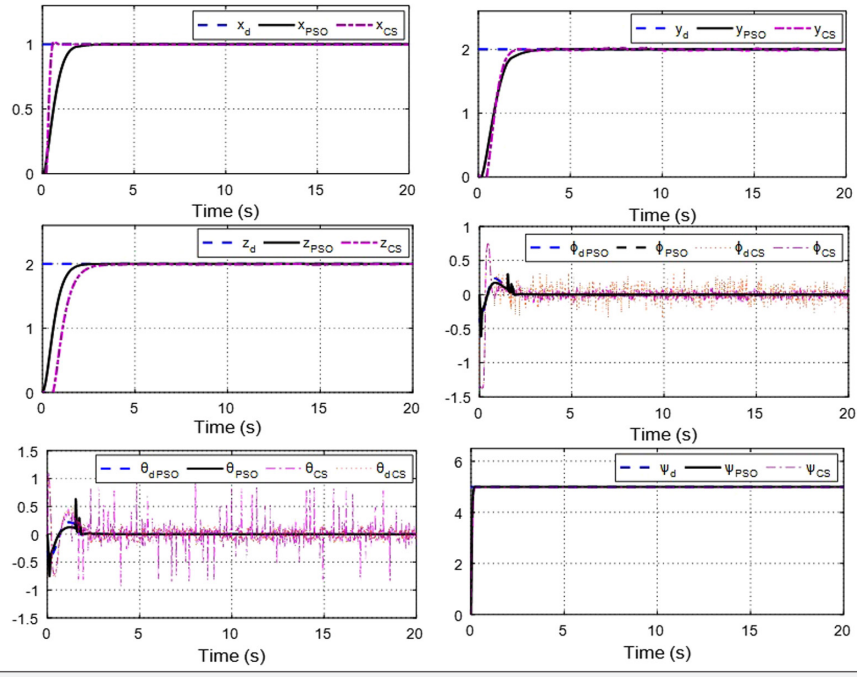

Fig. 5. Quadrotor's position (x, y, z) and attitude (ϕ, θ, ψ) during hovering by using CS and PSO. CS, cuckoo search; PSO, particle swarm optimization.

TABLE III. PERFORMANCE OF QUADROTOR RESPONSES OBTAINED PSO-SMC, CS, SMC, PSO-PID, CS-PID, PSO-CS-PD, GS-NNPID, AND GAHC-PID

Output	Performance	PSO-SMC	CS-SMC	PSO-PID [26]	CS-PID [26]	PSO-CS-PID [26]	GAHC-PID [28]	GS-NNPID [4]	NL PID [8]
ϕ	ISE_1	0.0079	0.0179	0.028	0.006	0.005	-	-	-
	RMS_1	0.0889	0,1338	0.1673	0.0774	0.0707	-	-	0.8205
θ	ISE_2	0.0172	0.0600	0.334	0.129	0.024	-	-	-
	RMS_2	0.1311	0,2449	0.5779	0.3592	0.1549	-	-	1.0532
ψ	$T_{s\psi}$ (s)	0.1191	0.1574	0.172	0.207	0.097	-	-	-
	$M_{p\psi}$ (%)	0	0	0.300	20.424	0.047	0	0	-
	ISE_3	0.7333	1.0196	0.036	0.037	0.022	0.3	0.16	-
	RMS_3	0.8563	1,0097	0.1897	0.1923	0.1483			0.2564
x	M_{ps} (%)	0.0391	2.1302	0.412	1.769	0.446	0	0	-
	T_{sx} (s)	1.2937	0.4948	0.730	1.384	0.522	-	-	-
	ISE_4	0.7333	0.3018	0.227	0.346	0.1650	2.2	1.36	-
	RMS_4	0,8563	0.5494	0.4764	0.5882	0,4062	-	-	0.0268
y	M_{py} (%)	0.0253	0.2137	0.497	0.898	0.010	0	0	-
	T_{sy} (s)	1.2887	1.5784	0.675	1.018	0.782	-	-	-
	ISE_5	2.3509	2.8501	0.237	0.296	0.226	2.5	1.5	-
	RMS_5	1,5333	1,6882	0.4868	0.5440	0,4754	-	-	0.0312
z	M_{pz} (%)	0.0027	0.4189	0.107	2.463	0.002	0	0	-
	T_{sz} (s)	1.0712	2.2025	1.070	1.821	0.813	-	-	-
	ISE_6	1.5974	3.4393	0.243	0.406	0.208	2.5	4.7	-
	RMS_6	1.2638	1.8545	0.4929	0.6372	0.4561	-	-	0.0193

CS, cuckoo search; GAHC, genetic algorithm hierarchical control; ISE, Integral Square Error; PID, proportional integral derivative; PSO, particle swarm optimization; RMS, root means square; SMC, sliding mode controller.

measured outputs ($x, y, z, \phi, \theta, \psi$), denoted as d_1, d_2, d_3, d_4, d_5, and d_6, with a time-dependent behavior represented as *sin (0.5t)*. Fig. 6 displays the four control signals (u_1, …, u_4), while Fig. 7 presents the tracking of desired trajectories using PSO-SMC and CS-SMC. Furthermore, the same figure illustrates the tracking in 3D plan using PSO-SMC both with and without the presence of external disturbances.

From the observations made in Fig. 5, it is evident that the control laws implemented with PSO-SMC (u_{1PSO}, u_{2PSO}, u_{3PSO}, u_{4PSO}) still present smooth variations. However, this contrasts with the behavior of CS-SMC controls (u_{1CS}, u_{2CS}, u_{3CS}, u_{4CS}), which demonstrates less smooth variations under the same conditions. In this test, the ability of PSO to ensure the aircraft stability is validated in presence of disturbances, as the error values have decreased in time and converged to zero in less than 2 seconds for the six outputs.

Fig. 7 provides compelling evidence of the remarkable capabilities of PSO-SMC in achieving precise control over various aspects of quadrotor flight. It demonstrates PSO-SMC ability to execute a complete circular trajectory flawlessly, closely track the desired altitude trajectory z, and maintain a precise 5° yaw attitude. The figure also illustrates the perfect tracking of desired roll and pitch signals (ϕ_d and θ_d).

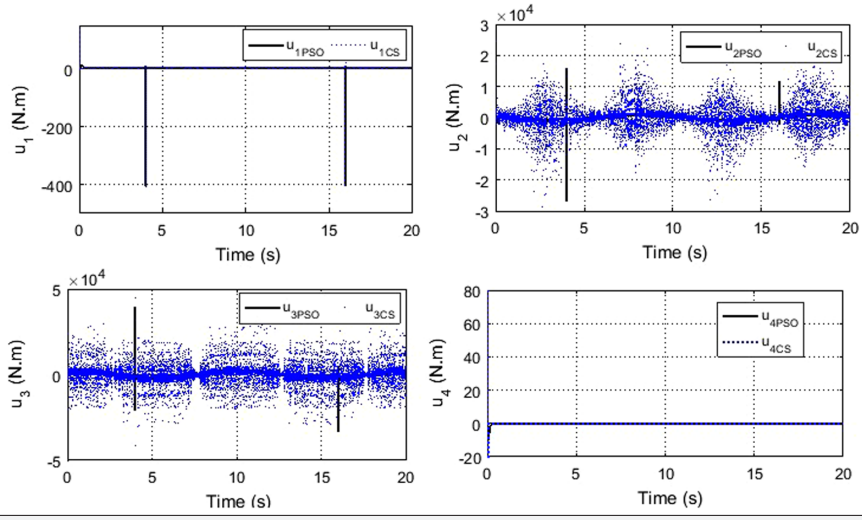

Fig. 6. PSO-SMC controls (u_{1PSO}, u_{2PSO}, u_{3PSO}, u_{4PSO}) and CS-SMC controls (u_{1CS}, u_{2CS}, u_{3CS}, u_{4CS}) for trajectory tracking.

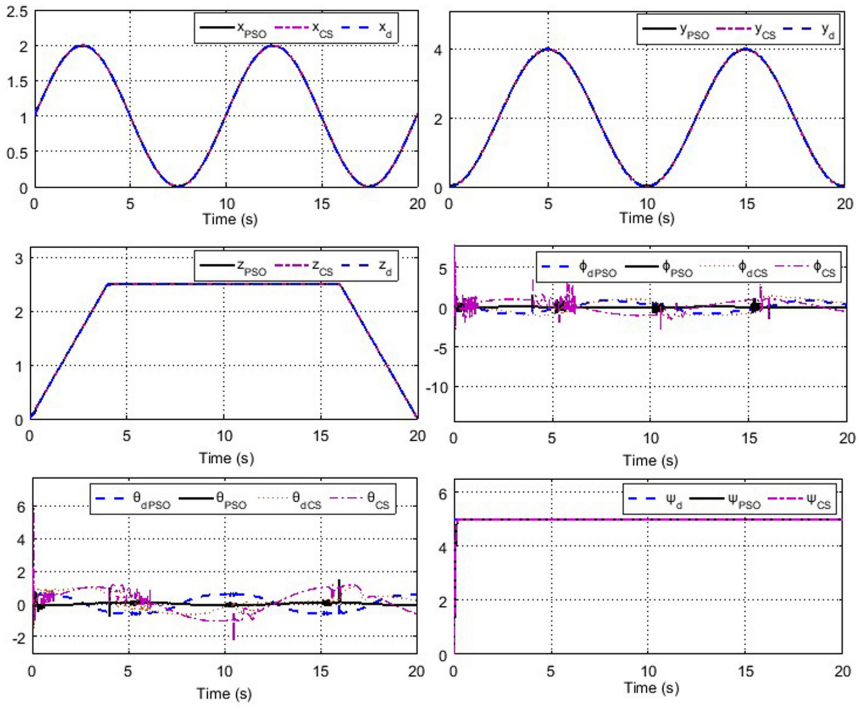

Fig. 7. Quadrotor's tracking position (x, y, z) and attitude (ϕ, θ, ψ) by using CS and PSO. CS, cuckoo search; PSO, particle swarm optimization.

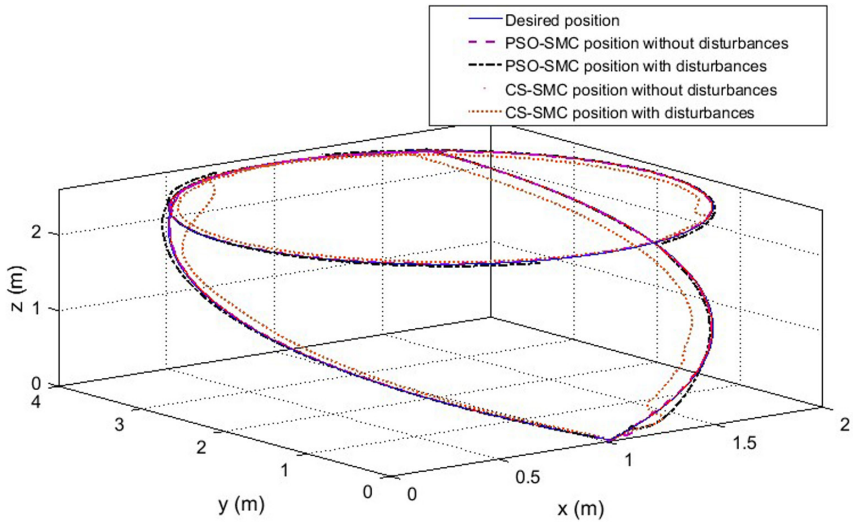

Fig. 8. Quadrotor's tracking position (x, y, z) in 3D plan using PSO-SMC and CS-SMC with/without disturbances injection. CS, cuckoo search; PSO, particle swarm optimization; SMC, sliding mode controller.

Furthermore, when examining the quadcopter's trajectory tracking in 3D plan, as shown in Fig. 8, it becomes clear that CS-SMC exhibits deviations in its trajectory when external disturbances are present. In contrast, PSO-SMC maintains a consistent trajectory even in the face of external disturbances. These findings not only highlight the superiority of PSO-SMC in achieving precise trajectory tracking for all variables (position (x, y, z) and orientation (ϕ, θ, ψ), but also underscore its rapid response, excellent tracking capabilities, and its ability to effectively reject the effects of external unknown disturbances. Moreover, PSO-SMC significantly mitigates the well-known chattering effect, ensuring stable attitude control with smoother variations and reduced control switching.

VI. CONCLUSION

An adaptive SMC structure based PSO and CS algorithms, has been successfully applied in this work for optimal full control of quadrotor during trajectory tracking missions. The proposed PSO and CS algorithms efficiently compute the requisite control signals to determine the optimal SMC parameters. Consequently, the control law has been derived in the sense of the Lyapunov theory and the stability of the closed loop has been rigorously established. The attained stability ensures that the quadrotor maintains a stable attitude while performing hovering, take-off, and landing maneuvers, thereby demonstrating the controllers' effectiveness in achieving precise trajectory tracking, even in the presence of unknown disturbances effects.

Finally, a comprehensive comparison of the outcomes obtained through the proposed PSO-SMC and CS-SMC approaches against those generated by intelligent PIDs, including cooperation PSO-CS-PID, genetic algorithm hierarchical control, hybrid neural networks, fuzzy PID controllers (FPID), and FPID (FPID-PSO), conclusively establishes the superiority of the proposed PSO-SMC in terms of adaptability and robustness. This approach exhibit potential applicability across a broad spectrum of nonlinear systems, effectively addressing the challenges posed by external disturbances.

Peer-review: Externally peer-reviewed.

Author Contributions: Concept – N.E.G.; Design – N.E.G.; Supervision – M.M., A.E.K., H.A.; Data Collection and/or Processing – N.E.G., K.E.H.; Analysis and/or Interpretation – K.E.H., M.M.; Literature Review – M.M.; Writing – N.E.G.; Critical Review – M.M., A.E.K., H.A.

Declaration of Interests: The authors have no conflict of interest to declare.

Funding: The authors declared that this study has received no financial support.

REFERENCES

1. N. El Gmili, "Unmanned Aerial Vehicles Control Systems by exploiting the Particle Swarm Optimization Method." PhD thesis, UCA Marrakech, 2020.
2. C. Kang, B. Park, and J. Choi, "Scheduling PID attitude and position control frequencies for time-optimal quadrotor waypoint tracking under unknown external disturbances," *Sensors (Basel)*, vol. 22, no. 1, p. 150, 2021. [CrossRef]
3. K. El Hamidi, M. Mjahed, A. El Kari, and H. Ayad, "Neural and fuzzy based nonlinear flight control for an unmanned quadcopter," *IREACO*, vol. 11, no. 3, pp. 98–106, 2018. [CrossRef]
4. K. E. Hamidi, M. Mjahed, A. E. Kari, and H. Ayad, "Quadcopter attitude and altitude tracking by using improved PD controllers," *Int. J. Nonlinear Dyn. Control.*, vol. 1, no. 3, pp. 287–303, 2019. [CrossRef]
5. I. Lopez-Sanchez, and J. Moreno-Valenzuela, "PID control of quadrotor UAVs: A survey," *Annu. Rev. Control*, vol. 56, p. 100900, 2023. [CrossRef]
6. G. V. Raffo, M. G. Ortega, and F. R. Rubio, "Nonlinear H∞ Controller for the Quad-Rotor Helicopter with Input Coupling," *IFAC Proc. Volumes*, vol. 44, no. 1, pp. 13834–13839, 2011. [CrossRef]
7. M. A. M. Basri, A. R. Husain, and K. A. Danapalasingam, "Enhanced backstepping controller design with application to autonomous quadrotor unmanned aerial vehicle," *J. Intell. Robot. Syst.*, vol. 79, no. 2, pp. 295–321, 2015. [CrossRef]
8. J. Moreno-Valenzuela, R. Pérez-Alcocer, M. Guerrero-Medina, and A. Dzul, "Nonlinear PID-type controller for quadrotor trajectory tracking," *IEEE ASME Trans. Mechatron.*, vol. 23, no. 5, pp. 2436–2447, 2018. [CrossRef]
9. Z. Hou, X. Yu, and P. Lu, "Terminal sliding mode control for quadrotors with chattering reduction and disturbances estimator: Theory and application," *J. Intell. Robot. Syst.*, vol. 105, no. 4, p. 71, 2022. [CrossRef]
10. Y. Shtessel, C. Edwards, L. Fridman, and A. Levant, *Sliding Mode Control and Observation*. New York: Springer, 2014.

11. X. Shi, Y. Cheng, C. Yin, S. Dadras, and X. Huang, "Design of fractional-order backstepping sliding mode control for quadrotor UAV," *Asian J. Control*, vol. 21, no. 1, pp. 156–171, 2019. [CrossRef]
12. N. Wang, Q. Deng, G. Xie, and X. Pan, "Hybrid finite-time trajectory tracking control of a quadrotor," *ISA Trans.*, vol. 90, pp. 278–286, 2019. [CrossRef]
13. M. Labbadi, and M. Cherkaoui, "Novel robust super twisting integral sliding mode controller for a quadrotor under external disturbances," *Int. J. Dyn. Control*, pp. 1–11, 2019.
14. W. Wu, X. Jin, and Y. Tang, "Vision-based trajectory tracking control of quadrotors using super twisting sliding mode control," *Cyber Phys. Syst.*, vol. 6, no. 4, pp. 207–230, 2020. [CrossRef]
15. N. Nafia, A. El Kari, H. Ayad, and M. Mjahed, "Robust full tracking control design of disturbed quadrotor UAVs with unknown dynamics," *Aerospace*, vol. 5, no. 4, p. 115, 2018. [CrossRef]
16. H. Razmi, and S. Afshinfar, "Neural network-based adaptive sliding mode control design for position and attitude control of a quadrotor UAV," *Aerosp. Sci. Technol.*, vol. 91, 12–27, 2019. [CrossRef]
17. L. Ding, and Y. Li, "Optimal attitude tracking control for an unmanned aerial quadrotor under lumped disturbances," *Int. J. Micro Air Veh.*, vol. 12, 2020. [CrossRef]
18. L. Ding, R. Ma, Z. Wu, R. Qi, and W. Ruan, "Optimal joint space control of a cable-driven aerial manipulator," *CMES Comput. Model. Eng. Sci.*, vol. 135, no. 1, 441–464, 2023. [CrossRef]
19. J. Kennedy, and R. C. Eberhart, "Particle swarm optimization", Proceeding of the IEEE international conference on neural networks, Perth, Australia, 19421948, 1995. [CrossRef]
20. A. S. Joshi, O. Kulkarni, G. M. Kakandikar, and V. M. Nandedkar, "Cuckoo search optimization-A review," *Mater. Today Proc.*, vol. 4, no. 8, pp. 7262–7269, 2017. [CrossRef]
21. S. Chaine, and M. Tripathy, "Design of an optimal SMES for automatic generation control of two-area thermal power system using cuckoo search algorithm," *J. Electr. Syst. Inf. Technol.*, vol. 2, no. 1, pp. 1–13, 2015. [CrossRef]
22. N. El gmili, M. Mjahed, A. El kari and H. Ayad, "An Improved Particle Swarm Optimization (IPSO) approach for identification and control of stable and unstable systems". *Int. Rev. Autom. Control*, vol. 10, no. 3, pp. 229–239, 2017.
23. A. A. Zamani, S. Tavakoli, and S. Etedali, "Fractional order PID control design for semi-active control of smart base-isolated structures: A multi-objective cuckoo search approach," *ISA Trans.*, vol. 67, pp. 222–232, 2017. [CrossRef]
24. N. H. Abbas, and A. R. Sami, "Tuning of PID Controllers for Quadcopter System using Hybrid Memory based Gravitational Search Algorithm–Particle Swarm Optimization," *Int. J. Comput. Appl.*, vol. 172, pp. 80–99, 2018.
25. N. El Gmili, M. Mjahed, A. Elkari, and H. Ayad"Improved cuckoo search approach based optimal proportional-derivative parameters for quadcopter flight control" *Aust. J. Electr. Electron. Eng.*, vol. 19, no. 3, pp. 219–232, 2022. [CrossRef]
26. N. El Gmili, M. Mjahed, A. El Kari, and H. Ayad, "Particle Swarm Optimization and Cuckoo Search-Based Approaches for Quadrotor Control and Trajectory Tracking" *Appl. Sci.*, vol. 9, no. 8, p. 1719, 2019. [CrossRef]
27. S. Bouabdallah, *Design and Control of Quadrotors with Application to Autonomous Flying*. Doctoral dissertation. Ecole Polytechnique Federale de Lausanne, 2007.
28. I. Siti, M. Mjahed, H. Ayad, and A. El kari, "New trajectory tracking approach for a quadcopter using genetic algorithm and reference model methods," *Appl. Sci.*, vol. 9, no. 9, p. 1780, 2019. [CrossRef]

Nada El Gmili obtained her PhD from the Cadi Ayyad University of Morocco in 2020, and a state engineeing degree from the National School of Applied Sciences (ENSA) of Oujda of Morocco in 2014. She has a previous experience of teaching at the Faculty of Sciences and Techniques (FST) of Marrakesh, Morocco from 2017 to 2020, and from 2020 she became a professor at the FST of Mohammedia, Hassan II University, Casablanca, Morocco. Her research interests include robotics, automatics, intelligent optimization, artificial intelligence, embedded systems, and mathematical modeling of complex systems. Her research results have been crowned by several publications indexed in the international Thomson Reuters and Scopus databases.

Khadija El Hamidi pursued her PhD in electrical engineering at Cadi Ayyad University in Marrakech, Morocco, in 2020. She also holds a master's degree in electrical engineering from the same university, which she completed in 2014. Her research focuses on the intersection of robotics, controls, and machine learning. Her goal is to enhance the performance, safety, and autonomy of quadcopters. She has published several papers in indexed journals and conferences in recent years, with her professional and research experience focus on diverse field of electrical engineering science including robotics, unmanned aerial vehicles, artificial Intelligence, automatic, identification, and modlling systems.

Mostafa Mjahed received his third cycle doctorate in HEP from the University of Clermont Ferrand, France, in 1987, and a PhD degrees in Control and Artificial Intelligence from the University of Cadi Ayyad, Marrakech, in 2003. In 1989, he joined the Ecole Royale de l'Air, Marrakech, Morocco, as an associate professor in the Department of Mathematics and Systems. From 2003, he has been a professor in the same institute and department. His current research interests are conventional and AI based flight control, pattern recognition and classification by GA, PSO, and NN.

Abdeljalil El Kari obtained his doctorate thesis in 1993 form University of Bordeaux I. Since 1994, he is a professor at the Faculty of Science and Technology of Marrakech, responsible of electrical engineering master. In 2002, he obtained the PhD degrees from Cadi Ayyad University and Reims Champagne-Ardenne University. He is a researcher member of the Electric Systems and Telecommunications Laboratory. His research interests concern automatics, robotics, and artificial intelligence.

Hassan Ayad obtained his doctorate thesis in 1993 form University of Le Havre, France, and the PhD degrees from Cadi Ayyad University in 2007. Since 1993, he is a professor at the Faculty of Science and Technology of Marrakesh, Responsible of the Physical department. He is a researcher member of the Electric Systems and Telecommunications Laboratory. He has participated in and led several research and cooperation projects and he is the author of more than 20 international communications and publications.